DRAFT!!! LAMA Memo 803
Simulation of Atmospheric Phase Correction Combined With Instrumental Phase Calibration Using Fast Switching

M.A. Holdaway and L. D'Addario
National Radio Astronomy Observatory
949 N. Cherry Ave.
Tucson, AZ 85721-0655
email: mholdawa@nrao.edu

November 25, 2003

Abstract

The BEST EVER evaluation of fast switching.

1 Introduction

1.1 Phase Errors are Really Bad

Phase fluctuations due to the atmosphere are really bad. If unchecked, they will result in:

- decorrelation, which means a loss of sensitivity.
- the decorrelation will actually be variable, leading to visibility amplitude flucuations. These in turn will complicate the flux calibration and limit the image quality.
- phase errors, which basically limit our ability to determine where anything really is, messing up our images and limiting our resolution.

Chajnantor may be one of the best millimeter and submillimeter sites in the world, but let me let you in on a little secret: the median phase stability on Simon Radford's 300 m basline interferometer indicates that if we were to ignore phase calibration at 230 GHz on that same 300 m baseline, the coherence would only be 0.5! Thats more than half of ALMA's sensitivity down the drain for the worst half of the time, at relatively low frequencies of 230 GHz and relatively short baselines of 300 m. Remember this: Chajnantor is an excellent site as judged by transparency, but when you look at the phase stability, ALMA is only marginally better than other sites.

Yes, phase errors are really bad.

The statistical nature of the phase fluctuations is well understood – every ten minutes, we determine the phase structure function from the site testing interferometer data, which permits us to calculate the phase errors on any desired time or spatial scale, at any observing frequency. We have trouble extrapolating far beyond the 300 m baseline which the site testing interferometer measures, as the phase structure function is expected to flatten somewhere around 500 or 1000 m – depending upon the thickness of the turbulent atmospheric layer. However, as we can see, if you are worried about what the phase structure function is doing at 1000 m, you've already lost the war. All the action is down on short time and spatial scales.

1.2 But Phase Errors Can be Corrected

Of course, we've been worrying intensely about the problem of phase correction on ALMA for over a decade, and it is widely appreciated that we must win the battle for phases at the shortest possible time scales.

The two competing correction methods are WVR ((get references)), which will perform well on time scales as short as 1 sm but has problems tying in the fluctuations to absolute water vapor levels (ie, has trouble with the long scales) – and FS, which, with typical switching time scales of 20 seconds, will effectively remove atmospheric structure on time scales of about 10 seconds, and has no problems hooking into longer time scales.

The BIG hope is that these two seemingly complimentary phase compensation methods might work together as a coherent phase compensation strategy, but constructing and verifying such a strategy requires either extensive simulations beyond our current capabilities, or an operating ALMA with which to experiment.

2 Overview of Fast Switching

2.1 Single Frequency Fast Switching

Fast switching phase calibration is a phase compensation strategy which solves for the atmospheric antenna-based phases by quickly observing a moderately bright point source calibrator and quickly rushes to the target source to oberve for a limited integration. However, as the atmosphere changes and the calibrator phase solutions go stale, we must go back and observe the calibrator again. With the nearly complete record of atmospheric phase stability data from Simon Radford's site testing campaign at Chajnantor, and our detailed understanding of the fast switching phase calibration process, we can calculate fairly precisely how often we must observe that calibrator and how much sensitivity we will lose by calibrating instead of observing, and how much sensitivity will be lost due to decorrelation from the imperfectly calibrated phases. While there are many populations of sources which could serve as phase calibration sources, we think that the quasars will provide a good combination of being both ubiquitous and unresolved.

Fast switching has been shown to work at several millimeter observatories. It is generally accessible to all telescopes, as it is little more than traditional phase and amplitude calibration, only done on time scales short enough to actually track some or most of the atmospheric fluctuations. However, as no telescope before ALMA has been designed with fast switching in mind, on existing telescopes, we take what the telescope provides in terms of calibration strategies. On ALMA, we expect to see a highly tuned version of fast switching achieve the most we can, given what nature provides us in terms of the atmospheric conditions and the sky full of calibration sources.

2.2 Cross Band Fast Switching

But ALMA will go yet another step beyond what existing telescopes are able to do: it is planned that ALMA will perform the phase calibration at the relatively low and sensitive frequency of 90 GHz and scale the phases, presumed due to non-disperive atmospheric delays, up to the observing frequency. Our past calculations of ALMA's fast switching efficiency have appreciated the fact that the phase solutions at the lower frequency have to be very accurate in order to scale them to the target frequency. While we knew we would need to periodically observe a bright calibrator at both the calibrator and target frequencies to solve for the instrumental phases at both frequencies, we have never calculated the impact this so-called cross-band calibration or instrumental sequence would have on fast switching efficiency. We needed an estimate of the brightness of the calibration sources as a function of frequency, and it wasn't until now that the urgency of the impending detailed system specifications has driven us to make such estimates. In order to more accurately predict the efficiency of fast switching phase calibration on ALMA, we also need to make progress in measuring the source counts of potential ALMA calibrators at higher frequencies.

2.3 The Fast Switching Schematic

We present a rather detailed picture of the sequence of observing operations that will be required of ALMA in cross band fast switching phase calibration in Figure 1. This figure shows a cross-band calibration (or instrumental sequence), a moderate number of fast switching cycles, and, before the instrumental phase has drifted significantly, a final cross-band calibration. We call this a single major cycle, though it is also logically a cross band cycle. The major cycle time is set by the instrumental stability time scale, which we assume in this work to be 300 s. This work will define just how much the instrumental phase can drift over a major cycle, and ALMA's actual instrumental phase stability will, in the future, instruct us in how long we can make the major cycle and still achieve small enough instrumental phase drifts. Of course, we hope the instrumental stability time scale is longer than 300 s, as it should be at moderate to low frequencies. If the instrumental stability time scale is longer, our work is still valid as lower limits for the overall fast switching efficiencies.

Conceptually, we start before the observations start. We must have good knowledge of the fluxes and positions of potential calibrator sources. Given such a database, possibly updated with recent observations to provide current fluxes, we determine the optimal calibrators for both the fast switching calibration and the cross-band or instrumental sequence.

Consider this overview of a single 300 s major cycle. During this 300 s cycle, we perform a short (10-25s) cross band phase calibration on a bright (ie, 0.5 - 1.0 Jy) and relatively distant (5-15 deg) calibrator, followed by several (10-20) cycles of fast switching phase calibration, alternating between the target source and a very close ($<$ 2 deg) moderately bright (0.05 - 0.2 Jy) phase calibrator. In the schematic, observations at the target frequency are unshaded, observations at the calibration frequency are shaded black, and slewing is shaded with diagonal lines. The majority of the time is spent on the target source at the target frequency. The calibrator observations in each fast switching cycle are very short, and the cross-band calibrations which bracket the 300 s observing segment are also very short.

In the cross-band (instrumental) calibration sequence, we begin by slewing to the really bright calibrator source which we must acurately detect at both the cal and the target frequencies. This source must be quite bright so we can detect it at both the calibrator and the target frequencies before the atmosphere has had a chance to change much. This source can easily be detected with sufficient SNR at the calibration frequency in 1 s. It will take 1.5 s to change to the target frequency. As we are racing the atmosphere and we don't have to change sky positions, any reduction in the time required to switch frequencies will be beneficial – in fact, the atmospheric error made in this step will ultimately set the requirements on the magnitude of the acceptable long-term electronic phase drift. Often, this source will also be bright enough to adequately detect the phase in a single 1 s integration at the target source, in which case it is time to slew to the fast switching phase calibrator and change back to the cal frequency. If the cross-band phase calibrator is not bright enough, we will need to switch back and forth between cal frequency observations and target frequency observations until we optain high enough SNR on the phase solutions at the target frequency. We perform this frequency switching on the cross-band calibrator to remove the contribution of atmospheric phase errors on time scales greater than about 2 s, essentially calibrating the target frequency observations of the instrumental calibrator with the cal frequency observations of the same source.

In a single fast switching cycle, we start with a short calibration observation at the calibration frequency. The integration time on the calibrator is determined by the calibrator's strength, ALMA's sensitivity, and the signal-to-noise ratio (SNR) required to scale the calibrator's phase solutions to the target frequency and still have errors which are less than the residual atmospheric phase errors. In all of our simulations, this is always less than a second.

Then we slew from the calibrator to the target source. The specification for antenna motion is 1.5 deg in 1.5 s, which is a typical distance to a calibrator. Furthermore, the specification on the setup time to change frequencies is 1.5 s, which will happen during the slew. In our modelling of the antenna slewing, it appears that very short slews (like 0.25 deg) might be completed in somewhat less than 1.5 s, so if we are able to change frequencies in less than a second, we'll take advantage of that capability. After slewing onto the target source with a specified pointing error of less than 3 acrsec (which will probably not be acceptable for very high frequencies or mosaicing – more on this topic below), we begin the actual observations on the target source at the target frequency. After integrating on source at the target frequency for 10-25 s, which is determined by a global optimization of the entire fast switching phase calibration procedure considering the current atmospheric conditions, the characteristics of the optimal calibrator, and the cal and target frequencies, we again slew back to the calibrator, and as we reach the calibrator, here ends a single fast switching cycle. Most often, we would immediately repeat this fast switching cycle with another one, starting on the phase calibrator again. If this is the last fast switching cycle before another cross band calibration, we should throw in a final observation of the calibrator to facilitate phase interpolation. If we are about to end the source block, or go off and do another sort of calibration, we should throw in a final cross-band calibration to facilitate in interpolating the scaled instrumental phase difference.

2.4 What About Fast Switching While Mosaicing?

ALMA antennas have an 0.65 arcsec pointing error specification to permit accurate mosaic imaging. What is the logic behind the 3 arcsec pointing specification for fast switching? It was originally reasoned that fast switching would do little to improve phase fluctuations on baselines shorter than 200 m (ie, $vt/2 + d$), and further reasoned that most mosaicing would be performed in the compact configurations with baselines less than 200 m. In these short configurations, the native phase stability of the atmosphere would permit observations without

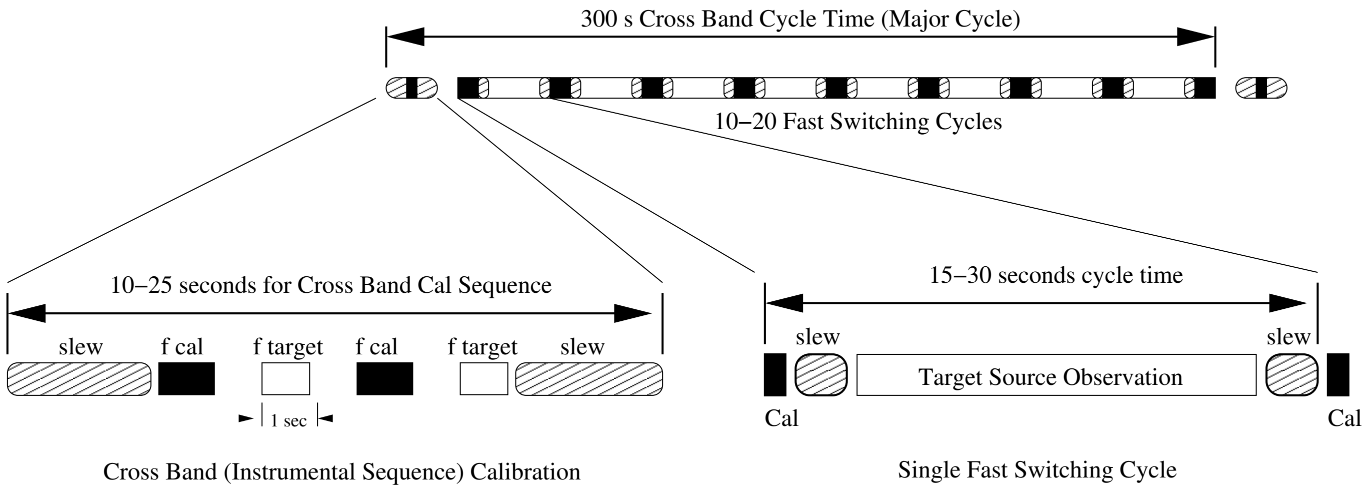

Figure 1: Overview of fast switching and the cross band calibration.

fast switching.

However, since conceiving of this fast switching spec, ALMA has grown in collecting area, and the smallest configuration is almost 200 m, while the effective switching scales can indeed be less than 200 m. Furthermore, often mosaics will be made in larger configurations which do require phase calibration. What can we do?

We do not have a spec for how long it will take ALMA antennas to settle to the 0.65 arcsec pointing level after fast switching, so we will have to study the antenna's settle down capabilities carefully to address this issue. Basically, when mosaicing and fast switching simultaneously, we will probably need to wait longer while the antennas slew to the target source to permit them to achieve better pointing. How much better pointing and how long will depend upon the required mosaic image quality, and in turn, on the mosaic's SNR. The time lost to waiting for the antennas to achieve superior pointing for mosaicing has not been included in the analysis of the fast switching efficiency, but should be included after we have studied this issue on the prototype antennas.

2.5 What About Fast Switching While Observing at Sub-millimeter Wavelengths?

The same issue will cloud our observations of sub-millimeter wavelength sources. Even single pointing sub-millimeter observations will require excellent pointing on the target source, so more time will be lost waiting for the antennas to settle to the desired pointing, which will depend upon both the observing frequency and the required image quality.

2.6 Defining Terms

We define the following terms in reference to Figure 1. Most of these terms will appear in the simulation results section.

- **fast switching tcal** is the time integrating on the weaker fast switching calibrator.

- **fast switching tslew** is the time it takes to slew from the target source to the fast switching calibrator source, or twice the frequency change time if it is longer than the slew time.
- **fast switching ttarget** is the time spent on the target source at the target frequency in a single fast switching cycle.
- **fast switching toverhead** includes both fast switching tcal and 2 * tslew, there and back, between the target source and the fast switching calibrator source.
- **fast switching tcycle** is the fast switching ttarget plus the fast switching toverhead, the time for a single complete cycle.
- **fast switching duty cycle** is the fast switching time on source divided by the fast switching cycle time.
- **fast switching eff1** is the efficiency due only to time lost from the target source during one fast switching cycle, and is given by the square root of the duty cycle.
- **fast switching effective baseline** is defined as $vt/s + d$, where v is the atmospheric velocity and t is the cycle time, and d is the distance between lines of site to the source and the calibrator. This will be dealt with in more detail later.
- **fast switching atmophase** σ_ϕ^a is the atmospheric component of the fast switching residual phase error at the target frequency, and is approximately equal to the phase structure function evaluated at the fast switching effective baseline. This will be dealt with in more detail later.
- **fast switching gainerror** is the error made in the gain phases, at the target frequency, due to finite SNR on the fast switching calibrator.
- **fast switching phase** σ_ϕ is the total phase error, rms, made by the fast fast switching cycles, and is equal to the sum in quadrature of the atmophase and the gainerror.
- **fast switching eff2** is the efficiency of the calibration process due to the fast switching phase errors, and is just the coherence given by

  $$eff2 = e^{-\sigma_\phi^2/2},$$

  with σ_ϕ being the fast switching phase (due to atmosphere and gain errors) in radians of phase at the target frequency.
- **fast switching eff0** is the product of fast switching eff1 and eff2. As the fast switching overhead time is determined by antenna capabilities and our need for accurate phase solutions, lengthening the fast switching cycle time will increase eff1, but will result in larger residual phase errors and lower eff2. As the cycle time decreases, the opposite trends are in play. For very short cycle times, the overall fast switching efficiency eff0 is low as eff1 tends towards zero. For very long cycle times, eff0 is low as eff2 tends towards zero. In between, there is an optimal cycle time, which will depend upon the atmospheric phase fluctuations and all. ALMA should be programmed to dynaimcall determine the fast switching cycle time which optimizes the fast switching efficiency eff0.

- **fast switching calibrator flux and calibrator distance** are obvious, and apply to the distance from the target source to the fast switching calibrator.
- **cross band tcal** actually refers to the time spent integrating on the brighter cross-band calibrator at both the cal and target frequencies, and the time spent in between changing frequencies. We take this to be 4 s for every 1 s integration we need on the calibrator to achieve the required phase solution accuracy at the target frequency. Note that 4 s is not exactly right: we are assuming 1 s to change frequencies, and then it is either $4n - 1$ (n is the number of 1 s target frequency integrations) if we have the same number of integrations at the cal and target frequency, or $4n + 1$ if we do one more cal frequency integration. So we average.
- **cross band tslew** is the time spent slewing from the fast switching phase calibrator to the cross band calibrator source.
- **cross band ttarget** is the time spent performing fast switching cycles (rather than cross band calibration).
- **cross band toverhead** is the cross band tcal plus twice the cross band tslew.
- **cross band cycle time (major cycle time)** is the cross band ttarget plus the cross band toverhead and is defined to be 300 s, the supposed instrumental stability time scale, in this work.
- **cross band duty cycle** is the cross band time on source divided by the cross band cycle time.
- **cross band eff1** is the efficiency due only to time lost to the cross band sequence or toverhead, and is the square root of the cross band duty cycle.
- **scaled instrumental phase difference** Φ_i will be the instrumental phase at the target frequency minus the instrumental phase at the cal frequency scaled by the ratio of the frequencies:
$$\Phi_i = \phi_i(\nu_{target}) - \phi_i(\nu_{cal}) \cdot \nu_{target}/\nu_{cal}.$$
More will be said about this quantity later.
- **cross band atmophase** is the atmospheric contribution corrupting the scaled instrumental phase difference, and ends up being the root structure function evaluated at about 2 s.
- **cross band gainerror** is the error in the scaled instrumental phase difference Φ_i due to the influence of thermal noise on the gain phase determinations.
- **cross band phase** is the overal phase error in the determination of the scaled instrumental phase difference Φ_i, and is equal to the sum in quadrature of the cross band gain error and the cross band atmophase.
- **cross band eff2** is the efficiency of the cross band calibration process due to cross band phase errors, and is equal to the coherence due to the cross band phase errors.

- **cross band eff0** is the product of cross band eff1 and eff2, and is a measure of the overall efficiency of the cross band calibration.
- **cross band cal flux** is the flux of the cross band calibrator at the calibration frequency.
- **cross band target flux** is the flux of the cross band calibrator at the target frequency.
- **all eff1** is the efficiency due to time lost from the target source by both fast switching and cross band calibration.
- **all eff2** is the efficiency due to residual phase errors, both atmospheric and noise-like, from both fast switching and cross band calibration.
- **all eff0** is the overal efficiency of the fast switching and cross band calibration processes, and is equall to all eff1 times all eff2. We seek a fast switching and cross band strategy which optimize the quantity all eff0.

2.7 Preview of the Requirements Fast Switching Places on the ALMA System

From the shape of the overall fast switching calibration, we can infer that fast switching will place requirements on:

- the rate at which the antennas can go from target source to cal source.
- ALMA antennas' ability to settle to better than 3 arcsecond pointing errors in a reasonable amount of time (ie, much less than the fast switching ttarget).
- how quickly ALMA can reconfigure between the target frequency and the cal frequency.
- the ALMA system must not incurr any uncalibratable phase jumps as the the frequency changes from the target freqency to the cal frequency and back.
- the antenna, LO, and entire ALMA system must maintain phase stability among pointing positions on the sky which differ by as much as 15 degrees when the antenna go back and forth between the target source and the cross-band calibrator.
- the instrumental phase must drift by an amount less than the residual cross-band phase, a requirement which will be spelled out in detail further on.

3 Calibrator Source Count Estimates

Of course, in order to calculate the tcal (integration time on the calibrator) and the tslew (slew time to calibrator), we need to know a bit about the calibrator source counts.

3.1 What Sources Are Possible Calibrators?

The success of fast switching is dependent upon an adequate supply of moderately bright calibration sources close by to the target source. The main population of calibrators for fast switching is the flat spectrum quasars. SiO masers have been suggested, but there are probably not enough of them which are bright enough to make a significant impact on our need for calibrators (REF). Ultra compact HII regions have also been considered, but they are extended and there probably aren't enough either (REF). Recently, Butler has suggested using thermal dust emission from distant galaxies at high frequencies where they will dominate the sky (rather than calibrate submillimeter observations at 90 GHz), but these sources will be extended (approximately 1 arcescond), and are probably not suitable for phase calibrators most of the time. Hence, we restrict the analysis of calibrators to the flat spectrum quasars. Adding any other population of sources to the calibrator pool will only improve the efficiency of fast switching, so our work will stand as a valid lower limit to fast switching's performance.

Butler's work does raise an interesting question. If we perform the fast switching phase calibration at the same frequency as the target source observations, we bypass the cross-band calibration (and any associated errors). Logically, at low target frequencies where the quasar fluxes are high and the ALMA sensitivity is good, it should be optimal to perform the fast switching phase calibration at the target frequency. At high target frequencies where the quasar fluxes are falling and ALMA sensitivity is poor, it will be advantageous to perform the fast switching calibration at a lower frequency and scale the solutions to the target frequency. So, there will be a frequency below which we will perform the phase calibration at the target frequency, and above which we will perform the phase calibration at 90 GHz and scale the solutions up. What is that magic frequency?

The current work needs to investigate the quasar source counts at every ALMA band to assess the accuracy of the cross-band (instrumental sequence) calibration. We can also use this information to help us calculate the frequency above which is will be optimal to perform the fast switching phase calibration at 90 GHz.

3.2 Estimating Flat Spectrum Quasar Source Counts in the Millimeter and Sub-millimeter

Figure 2 shows the histogram of the spectral index ($S(\nu) \propto \nu^{-\alpha}$) distribution from 8 GHz to 90 GHz for the 367 flat spectrum quasars observed by Holdaway, Owen, and Rupen (1994). The 8 GHz core fluxes were measured by Patniak et al with the VLA in A array. The 90 GHz fluxes were measured at the NRAO 12 m. Under the assumption that any extended emission is steep spectrum and will be negligible at 90 GHz, we posit that this spectral index distribution describes the quasar cores. We found that the spectral index distribution did not depend upon the quasar flux, so we used all 367 quasars to determine a single spectral index distribution using Fiegelson's ASURV code.

We have also performed a two Gaussian fit to this histogram (dotted lines, the sum of which is the dashed line). The black boxes represent the integral of the summed Gaussian fit over the histogram boundaries, appropriately normalized for comparison to the histogram. Because the number of degrees of freedom in the fit (6) is about the same as the number of independent data points in the histogram (7), we expect a very good fit. We have used the Gaussian fit, rather than the 7 bin histogram, for our extrapolations of source counts to the higher frequencies, as the sharp edges were causing some odd bumps in the source counts extrapolations.

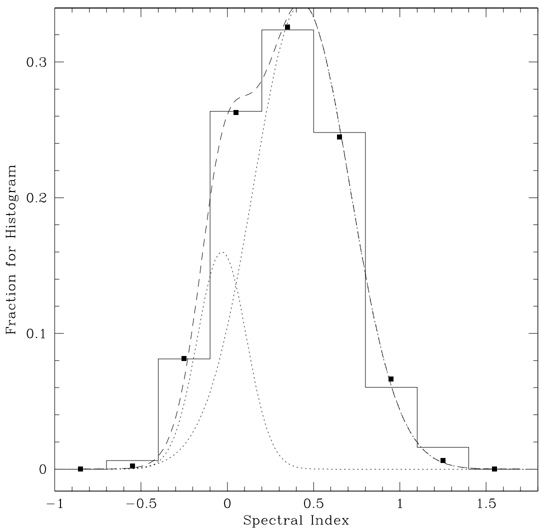

Figure 2: The seven bin histogram is the spectral index ($S(\nu) \propto \nu^{-\alpha}$) distribution from 8 GHz to 90 GHz for the 367 flat spectrum quasars observed by Holdaway, Owen, and Rupen (1994). See text if you want to know about the Gaussians and filled squares.

Starting with the source counts of flat spectrum quasars at 5 GHz from Condon's GB86 survey, we modulated the fluxes of these counts by the core fraction distribution of the 3CR2 flat spectrum sources, so that the modified counts represented the source counts of only flat spectrum cores, ignoring extended components. We further modulated the source counts by the flat spectrum quasar spectral index distribution between 8 GHz and 90 GHz which we determined, following the prescription by Condon et all (1986) to scale the source counts up to 90 GHz.

At frequencies above 90 GHz, the quasar cores are expected to become optically thin, which will result in a spectral steepening. Hence, for frequencies above 90 GHz, we assume that the sources have a spectral break and we steepen the entire spectral index distribution by 0.5 when estimating quasar source counts at frequencies above 90 GHz. The resulting integral source count estimates for a range of frequencies are shown in Figure 3.

We have written an AIPS++/glish tool, `sourcecountsim.g`, which performs the frequency scaling of the source counts and can simulate a calibrator field which is consistent with the estimated source counts and spectral index distribution. The `sourcecountsim.g` code is not part of the AIPS++ distribution, but can be obtained from Mark Holdaway's home page at `http://www.tuc.nrao.edu/ mholdawa/`

4 What Frequency Should We Calibrate At?

As mentioned above, the general scheme for fast switching is that we will calibrate at 90 GHz and scale the phase solutions up to the observing frequency. There are two issues which pertain to the assumption of calibrating at 90 GHz which we need to address now.

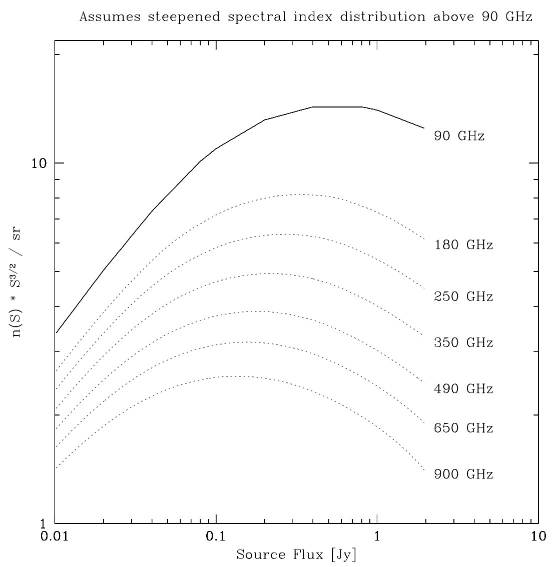

Figure 3: These are the integral source counts of flat spectrum quasars at various ALMA frequencies. The counts at 90 GHz will be fairly accurate, but we are guessing at the spectral index distribution for higher frequencies: to estimate the higher frequency source counts, we are taking the measured 8-90 GHz spectral index distribution and steepening it by 0.5.

4.1 Is 90 GHz the Optimal Calibration Frequency?

We have not examined this in detail yet (!), and we should, just to cover our bases. Band 3 is probably the best spot to do cross-band fast switching from, but nobody has ever shown this to be the case. Of course, if we do the calculations and prove it, we will be justifying *a postiori* a decision which has already been made, as the inclusion of 90 GHz for pointing observations and such is already a system level decision. We *have* investigated which frequency is optimal for pointing calibration at the ATF (Holdaway and Mangum, 2001), and the combination of the decent sensitivity and the "lever arm" of the smaller beam at the higher frequency makes 90 GHz superior to 30 GHz for pointing determinations. There are similar arguments for fast switching phase calibration that have not been entirely spelled out.

What about performing fast switching phase calibration at higher frequencies, like 140 GHz, and scaling up to the target frequency? Answering this question would probably be dominated by our assumptions about how the calibrator fluxes are falling down, and it is probably not worth investigating this question at this time.

When the final ALMA systems are in production and we understand the system temperature as a function of frequency, we can determine the optimal frequency band within band 3 for fast switching.

4.2 Potential Issues with Cross-Band Calibration Sources

We have asserted that the cross-band calibration, or instrumental sequence, will be performed on a quasar which is bright at both the calibrator frequency and the target frequency. The success of this strategy depends, among other things, on the quasar looking the same at the calibration and the target frequencies. This many not be the case.

For example, as dust emission increases in flux with frequency, the quasar point source may be surrounded by extended dust emission. The dust emission problem probably doesn't exist for moderate frequencies, perhaps only for frequencies of 400 GHz and above. Furthermore, if we are observing in a very large configuration, much of the dust emission could be resolved out – in other words, a (u,v) range could be determined observationally in which the calibration source was well approximated by a point source. Such a (u,v) range would eliminate some baselines from the phase solution, thereby requiring a brighter calibrator or more integrations on the calibrator.

Another potential problem is that the position of the quasar core will depend upon the frequency. As we observe at higher frequencies, the region at which the jet becomes optically thick (functionally "the core") will be closer and closer to the central engine. This would introduce a systematic error in the cross-band calibration. We need to investigate how large this systematic error might be.

4.3 Dispersive Phase, Dry Fluctuations, and Implications on the Calibration Frequency

We claim that we can scale the phase solutions from the calibrator frequency up to the target frequency simply by multiplying by the ratio of the frequencies. This is only true for target frequencies at which the atmosphere is non-dispersive, which is probably up to 350 GHz. However, at submillimeter wavelengths, the atmosphere is dispersive enough to result in significant deviations from this simple phase scaling. At the very least, we will be required to employ radiation transmission codes such as ATM to instruct us in the proper phase scaling from calibrator to target frequencies. However, we could be limited in the accuracy of the transmission codes, or we may be limited in our knowledge of physical atmospheric parameters such as the temperature profile or the temperature profile, which would result in some errors in our prescribed phase scaling. We can study the latter question now using ATM with various atmospheric profiles. However, in this memo we do not attribute any errors to the phase scaling process.

However, we must consider the possibility that the dispersive phase in the submillimeter range may not permit fast switching from scaling the phases from calibration to target frequency. If this were the case for certain frequencies, we would have to resort to performing the fast switching calibration at the target frequency and make do with the weaker or more distant phase calibrators. Later in this memo, we document how effective fast switching is at each target frequency.

While the dry component of the atmosphere results in the largest portion of the overall atmospheric delay, we expect that the dry atmosphere will be relatively stable and will contribute essentially none of the phase. If there are significant phase fluctuations introduced by fluctuations in the dry atmosphere, fast switching with different calibration and target frequencies will still work fine unless there is a significant dispersive phase. In other words, if there are dry phase fluctuations, we can calibrate at 90 GHz and scale the phase up to about 350 GHz, but we we can't scale the phase up to the submillimeter where the phase is despersive – basically, we would need to know how much of the phase errors are dry and non-dispersive and how much of the phase errors were wet and dispersive. So, if dry fluctuations were significant, we would probably need to perform fast switching phase calibration at the target frequency.

5 Analysis of Fast Switching Errors

Include Equations !! DO THIS SOON

5.1 RMS Phase Jitter, Phase Errors, and the Structure Function

To estimate the residual phase errors after fast switching, we have in the past used the expression

$$\sigma_\phi = \sqrt{D_\phi(v_{atmos} t_{cycle}/2 + d)}, \tag{1}$$

where σ_ϕ is the rms residual phase error, D_ϕ is the phase structure function determined by the site testing interferometer (Radford, ????; Holdaway et al, 1995), v_{atmos} is the atmospheric velocity, t_{cycle} is the fast switching cycle time, and d is the distance between the lines of sight to the target source and the calibrator. In the data analysis, we perform a power law fit to the root structure function, and parameterize it as

$$\sqrt{D_\phi(\rho)} = a \cdot \rho^\alpha,$$

where a is, in rough terms, the amplitude of the atmospheric phase fluctuations, and α is the root phase structure function power law exponent. (Our appologies for reusing the symbol α for both the quasar spectral index and the atmospheric structure function exponent, but the context should indicate which concept we are using.) The median value of α, for six years of site testing at Chajnantor, is 0.58.

In the term $v_{atmos} t_{cycle}/2 + d$, the d ends up being negligible: with v_{atmos}=12 m/s and t_{cycle}=20s, $vt/2$ will typicaly be 120 m. For a distance between calibrator and target source of 1 deg and a height of the turbulent layer of 500 m above the ground, d ends up being less than 10 m for a source at the zenith (lower elevation angles will make d somewhat larger). In the reasoning below, feel free to conceptually ignore d, although we did include d in the simulations.

The expression in Equation 1 systematically overestimates the residual phase error which will occur in fast switching. Figure 4 illustrates the problem. The top graph shows the simulated uncorrected atmospheric phase time series for a 1000 m baseline interferometer, and the lower graph shows the residual phase as a function of time on the target source after correcting with 2-point interpolation. Some time is lost due to slewing before and after the calibration observations.

With yet another AIPS++/glish tool, `vtdsim.g`, we have a laboratory to explore the finer details of fast switching and better determine the relationship between the residual phase, the phase structure function, and the effective fast switching baseline $vt/2 + d$. From perfoming such detailed simulations of fast switching and the statistics of the resulting residual phases, we have identified three effects which we need to address to more accurately gauge the success of our full blown simulated fast switching observations which are presented later in this memo:

- The rms residual phase error, given by the rms of the lower time series, will be a valid number for calculating decorrelation losses. However, the average phase error made on the target source visibility will be much smaller. In this case (more drastic than the

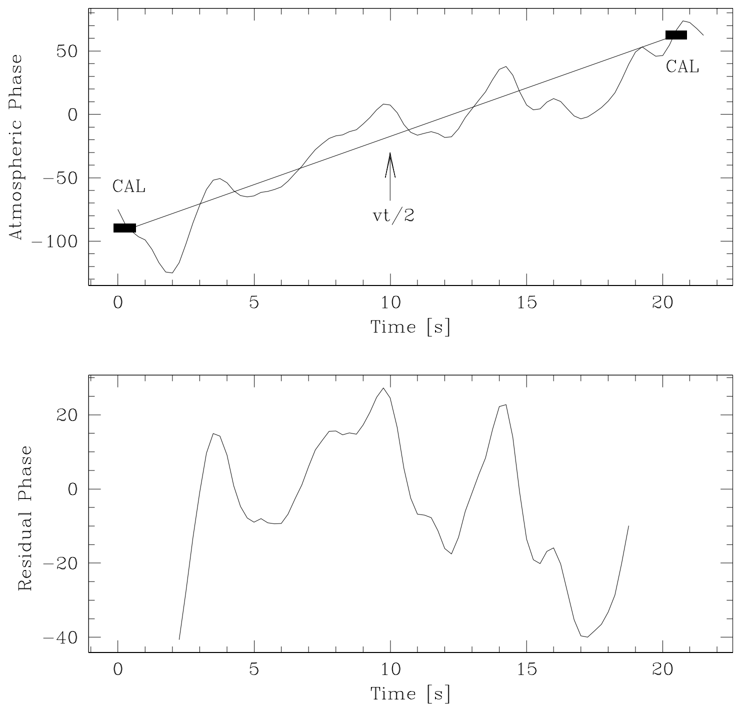

Figure 4: Most of the fast switching cycle will be closer to a calibration observation than $v_{atmos}t_{cycle}/2$. Hence, the phase errors will be somewhat less than $\sqrt{D_\phi(vt/2+d)}$; the d term is generally small compared to $vt/2$.

"average") the rms residual phase is 18 deg, while the mean phase error on this integration will be -4 deg. In our analysis, we will consider both the rms residual phase error for purposes of decorrelation calculations, and the rms of the average phases, for purposes of setting electronic phase stability requirements.

- For atmospheric α of 0.58, 2-point interpolation will provide a marginal improvement over a "closest calibrator" interpolation. For flatter α (ie, more like white noise), 2-point interpolation could actually be worse than closest calibrator interpolation, and for steeper α (ie, up to the maximum theoretical value of 0.83), 2-point interpolation should significantly reduce the residual phase.

- the rms phase error at the center of the target source integration (ie, 10 s, or $t_{cycle}/2$) might appropriately be estimated by the root structure function evaluate at $vt/2$, but most of the target source integration will be significantly closer to one or other calibration observations. In this particular case, the largest residual phase errors on the target source observation happen to occur at 2 s and at 17 s, near the calibrations. However, if we were to take the average of an ensemble of such observations, we would find stitistically that the points closer to calibration observations would have smaller residuals than the midpoint.

Including these three factors in simulations (mean vs rms phase, interpolation improvements, and $vt/2$ being the worst case), we find that simulated fast switching observations through a model atmosphere and 2-point interpolation, we find that the rms phase error is given by the phase structure function reduced by $\gamma_0(\alpha)$

$$\sigma_\phi = \gamma_0(\alpha) \cdot \sqrt{D_\phi(v_{atmos} t_{cycle}/2 + d)},$$

and the rms of the phase errors averaged over each target integration is given by the phase structure function reduced by $\gamma_1(\alpha)$

$$\langle \bar{\phi} \rangle = \gamma_1(\alpha) \cdot \sqrt{D_\phi(v_{atmos} t_{cycle}/2 + d)}.$$

We expect the γ factors to be weak functions of α, though at this time we have not performed exhaustive studies. For the simulations we performed, with $\alpha = 0.58$, and $t_{cycle} = 20$s, we find that $\gamma_0 = 0.65$ and $\gamma_1 = 0.35$

This is great news, that the mean phase errors are reduced by the factor of 0.35, and the rms phase errors are reduced by a factor of 0.65. However, we temper this with a bit of bad news.

If you observe with a single interferometer through the atmosphere with phase errors, the rms phase (after subtracting out the average phase) will increase with integration time until, after many "crossing times" (ie, the baseline length divided by the atmospheric velocity), the rms phase will saturate. When we worked out the site testing interferometer data reduction pathway (Holdaway et al, 1995), we performed this analysis, looking at how the rms phase increased with integration time. The rms phase reached a plateau at about 10 minutes, and then started to increase again for longer integration times. We interpreted this to mean that 10 minutes integration resulted in a saturated phased, and beyond 10 minutes, phase errors from thermal changes in the cables or satelite motion came into play.

However, our simulations with `vtdsim.g` indicate that a 600 s integration on a 300 m baseline and a 12 m/s wind is not really enough to reach saturation. When simulating a 300 m baseline interferometer with the `vtdsim.g` machinery, we find that the rms phase only accounts for about 0.70 of the phase structure function at 300 m. It is unclear if reanalysis of the site testing interferometer data using a longer integration time is the right thing to do, as non-atmospheric phase errors will creep in. For now, there is a very simple fix we can apply, and that is to incorporate this correction factor, 1/0.70, into the γ factors:

$$\gamma_0' = \gamma_0/0.70 = 0.93$$

$$\gamma_1' = \gamma_1/0.70 = 0.50$$

One more detail we must address is the way the phase errors will average down over several fast switching cycles. That γ_1' is 0.50 indicates that the average phase over a single switching cycle will be significantly lower than the rms phase. Typically, we will perform 10-20 such fast switching cycles, and, as the residual atmospheric errors after fast switching calibration are random, and the noisy gain errors on the fast switching calibrator are random, averaging the target source visibilities from several fast switching cycles will result in better and better estimates of the visibility phase. We assert that the ensemble average of the mean phase error after N_{cycles} fast switching cycles will actually go as

$$\langle \bar{\phi} \rangle = \gamma_1\prime(\alpha)/\sqrt{N_{cycles}} \cdot \sqrt{D_\phi(v_{atmos} t_{cycle}/2 + d)}.$$

This is very important in elucidating the requirement for the instrumental phase drift. As the full blown simulation results will show later, the rms phase fluctuations for high frequency observations might typically be 32 deg. Hence, the average phase error on a visibility integrated over a single fast switching cycle will be about 16 deg. If we average over 16 switching cycles in a major switching cycle, the phase error on that averaged visibility will be about 4 deg, which is really extremely low. We would like to set the specification on the electronic phase drift over the major cycle to permit us this improvement in the average phase error. However, we probably cannot take full advantage of this very small phase error, as the residual cross band atmospheric phase errors (the ones from the 2 s time scales in the cross band calibration) will typically be larger than the fast switching phases averaged over the major cycle. Hence, without proof at this moment, we assert that when we set the specification for the instrumental phase drift, we need to set it to be similar to the cross-band atmospheric phase error during some of the best phase conditions available on the Chajnantor site.

One final point concerning the number of visibilities which can be averaged is the crossing time of a visibility across a Nyquist sampled (u,v) cells due to earth rotation. The size of the (u,v) cells is set by the inverse of the field size we are imaging, and the number of cells will be proportional to the baseline length. Long baselines will zip across the (u,v) cells very quickly, short baselines will move through the cells slowly. The crossing time sets an upper limit to the amount of time one can average the visibilities for.

For full primary beam imaging, the (u,v) cell crossing times are given in Table 1.

Baseline [m]	t_{int} [s]	N_{cycles}	$\gamma_1'/\sqrt{N_{cycles}}$
200	412	20	0.11
400	206	10	0.16
1000	82	4	0.25
2000	41	2	0.35
4000	20	1	0.5
10000	8	-	-

Table 1: The (u,v) cell crossing time for full primary beam imaging, for a basine of the specified length, and the approximate number of fast switching cycles which could be averaged and the reduction factor in the phase error due to averaging. If only a portion of the primary beam were being imaged, the (u,v) cell sizes would be larger, the crossing time longer, and more averaging could take place, so these numbers represent a worst case.

6 Our Method of Calculating the Residual Phase Errors

6.1 This is a "squishy" sort of problem

Fast switching is a very complex multi-dimensional system. The variables that are out there include: the inherent sensitivity of the telescope, the distance to the calibrator, the strength of the calibrator, how much time we spend calibrating (multiply the last three dimensions by two, as there are both the fast switching calibrators and the cross band calibrators), how much time we spend observing our target source before we go back and observe the calibrator again, and the nature and level of the atmospheric phase fluctuations. With so many dimensions, the overal fast switching system becomes rather "floppy" – if one dimension of the problem becomes much harder (say we discover that the 90 GHz calibration sources are only half as bright as we had assumed), the impact of that change becomes absorbed in several dimensions (we go a little bit further away to reach a somewhat better calibrator, integrate a bit longer, shorten the overall cycle time, which decreases the on-target-source duty cycle), resulting in a final result, the overall observing efficiency, which is only marginally reduced.

The one exception to this seems to be the atmosphere. If you make the atmosphere twice as bad, the lost observing efficiency (due to both time lost to calibration and to phase decorrelation) gets twice as large.

6.2 Monte Carlo Simulations

DO THIS SOON

Hey, we simulated 1000 fields of calibrators, each with a different spectral index. The source counts at 90 GHz are consistent with what we know, the spectral index distribution is the one shifted by 0.5. For every different freq (atmos conditions, whatever), we use the same set of 1000 sources

Set atmospheric conditions to be the median conditions for that target frequency's bin, allocate the bins of conditions: 8best conditions to highest frequencies.

7 Results

We present the quantities that were defined in section 2.6, as calculated with our Monte Carlo simulations, in Tables 2 through 4. Table 5 deals with the 5th percentile antmospheric phase and opacity, and is dpecifically included so we can derive specifications for the electronic phase fluctuations. These tables show the median values of the various parameters calculated in the simulations.

The units of the quantities in these Tables are: targetfreq, calfreq [GHz], el [deg], rms300 (site testing phase) [deg], phases and gainerror [deg], calflux [Jy], caldist [deg], tslew, tcal, tcycle, ttarget, toverhead [seconds].

These tables are sort of sideways so many relevant terms can be shown. There are a number of interesting results:

- Things are really very demanding in the submillimeter, with typical overall efficiencies (all eff0) of under 0.70; total residual phase fluctuations are between 30 and 40 deg. Phase errors are about half of this.
- At millimeter wavelengths, the efficiencies are more like 0.76 and up to about 0.90 at the lowest frequencies; total residual phase fluctuations are between 20 and 30 deg. Phase errors are about half of this.
- Quite surprisingly, cross-band fast switching is only marginally more effective than single-frequency fast switching. Up to a target frequency of 345 GHz, calibrating at the target frequency is as efficient or more efficient than calibrating at 90 GHz, scaling the phases, and taking the extra time to perform the cross-band phase calibrator. Note that cross-band calibration would be somewhat more efficient if the electronic stability time scale were longer than 300 s.

The electronic stability specifications can be derived from the results in Table 5, which have been run for opacity and phase conditions corresponding to the best 5% of Chajnantor atmospheric conditions. We consider two different sorts of specifications: rms electronic delay jitter on timescales of a few tens of seconds (ie, the time scale of a single fast switching cycle), and the electronic delay drift on time scales of about 300 s.

For the delay jitter, the relevant parameter here is the “all phase” (or 0.93 time this phase). Converting these numbers to a delay results in 110 fs of delay jitter over a few tens of seconds.

We specify that the delay drift over 300 s be equal to the cross band delay error divided by two, as errors at two frequencies will come into this number. This ends up being about 40 fs of delay drift per band over 300 s.

HEY! We need to show the impact this will have over ALL bands. Make a graph.

8 References

Condon, GB86

Feigelson, E, ASURV.

targetfreq	850	850	650	650	490	490
calfreq	90	850	90	650	90	490
el	60	60	60	60	60	60
tau225	0.032	0.032	0.037	0.037	0.045	0.045
rms300	0.79	0.79	1.155	1.155	1.615	1.615
all phase	33.48	37.65	35.60	39.10	36.59	40.26
all eff0	0.719	0.678	0.704	0.663	0.695	0.648
all eff1	0.855	0.845	0.856	0.845	0.853	0.845
all eff2	0.842	0.805	0.824	0.792	0.815	0.781
cb eff0	0.944	1	0.947	1	0.945	1
cb eff1	0.962	1	0.969	1	0.969	1
cb eff2	0.981	1	0.977	1	0.974	1
fs eff0	0.764	0.678	0.744	0.663	0.737	0.648
fs eff1	0.894	0.845	0.881	0.845	0.881	0.845
fs eff2	0.858	0.805	0.843	0.792	0.836	0.781
fs calflux	0.140	0.0624	0.110	0.073	0.087	0.087
fs caldist	1.993	3.579	1.720	3.431	1.517	3.379
fs tslew	1.744	2.340	1.635	2.287	1.547	2.261
fs tcal	0.411	4.216	0.358	3.254	0.315	3.019
fs tcycle	19.84	29.46	17.44	24.98	16.19	23.62
fs ttarget	15.64	20.53	13.58	17.32	12.48	16.24
fs toverhead	4.131	8.453	3.858	7.402	3.618	7.277
fs phase	31.62	37.65	33.45	39.10	34.24	40.26
fs atmophase	31.22	37.32	33.08	38.78	33.87	39.95
fs gainerror	7.028	8.368	7.435	8.690	7.609	8.948
cb calflux	1.365	-1	1.256	-1	1.329	-1
cb tarflux	0.374	-1	0.372	-1	0.444	-1
cb caldist	13.44	0	11.57	0	11.47	0
cb tslew	6.633	0	5.602	0	5.645	0
cb tcal	8	0	4	0	4	0
cb tcycle	300	300	300	300	300	300
cb ttarget	277.7	300	282.0	300	281.8	300
cb toverhead	22.21	0	17.94	0	18.14	0
cb phase	11.08	0	12.34	0	13.02	0
cb atmophase	10.52	0	11.77	0	12.40	0
cb gainerror	3.509	0	3.924	0	4.136	0
same cal	0.036	0	0.038	0	0.029	0

Table 2: Median fast switching results for 850, 650, and 490 GHz, giving the best conditions to the high frequencies. Note that the second (fourth, sixth) columns are for the same target frequencies, but performing fast switching calibration at the target frequencies instead of 90 GHz.

targetfreq	345	345	230	230	190	190
calfreq	90	345	90	230	90	190
el	60	60	60	60	60	60
tau225	0.045	0.045	0.056	0.056	0.06	0.06
rms300	1.84	1.84	2.175	2.175	3.21	3.21
all phase	31.15	31.16	26.56	25.98	29.81	29.15
all eff0	0.766	0.768	0.818	0.829	0.786	0.794
all eff1	0.890	0.894	0.912	0.919	0.900	0.904
all eff2	0.862	0.862	0.898	0.902	0.873	0.878
cb eff0	0.968	1	0.976	1	0.972	1
cb eff1	0.984	1	0.986	1	0.986	1
cb eff2	0.984	1	0.990	1	0.985	1
fs eff0	0.792	0.768	0.839	0.829	0.809	0.794
fs eff1	0.904	0.894	0.925	0.919	0.912	0.904
fs eff2	0.876	0.862	0.907	0.902	0.886	0.878
fs calflux	0.078	0.060	0.068	0.049	0.054	0.052
fs caldist	1.399	2.254	1.298	1.678	1.163	1.624
fs tslew	1.491	1.853	1.428	1.612	1.365	1.596
fs tcal	0.262	0.521	0.209	0.330	0.193	0.318
fs tcycle	18.99	21.70	22.75	24.31	18.56	20.32
fs ttarget	15.46	17.15	19.42	20.56	15.45	16.56
fs toverhead	3.456	4.461	3.281	3.756	3.097	3.697
fs phase	29.40	31.16	25.29	25.98	28.12	29.15
fs atmophase	28.97	30.76	24.79	25.49	27.67	28.72
fs gainerror	6.533	6.925	5.621	5.773	6.249	6.479
cb calflux	0.388	-1	0.241	-1	0.205	-1
cb tarflux	0.144	-1	0.113	-1	0.118	-1
cb caldist	4.380	0	3.015	0	2.830	0
cb tslew	2.636	0	2.116	0	2.042	0
cb tcal	4	0	4	0	4	0
cb tcycle	300	300	300	300	300	300
cb ttarget	290.6	300	291.7	300	291.9	300
cb toverhead	9.361	0	8.260	0	8.084	0
cb phase	10.20	0	8.009	0	9.735	0
cb atmophase	9.954	0	7.844	0	9.563	0
cb gainerror	3.318	0	2.614	0	3.187	0
same cal	0.148	0	0.247	0	0.235	0

Table 3: Median fast switching results for 345, 230, and 190 GHz, giving the best conditions to the high frequencies. Note that the second (fourth, sixth) columns are for the same target frequencies, but performing fast switching calibration at the target frequencies instead of 90 GHz.

targetfreq	145	145	90	70	35
calfreq	90	145	90	70	35
el	60	60	60	60	60
tau225	0.089	0.089	0.129	0.129	0.22
rms300	2.955	2.955	3.635	5.44	6.71
all phase	23.83	23.14	19.35	21.26	15.90
all eff0	0.847	0.861	0.899	0.880	0.930
all eff1	0.924	0.935	0.953	0.942	0.967
all eff2	0.917	0.921	0.944	0.933	0.962
cb eff0	0.979	1	1	1	1
cb eff1	0.987	1	1	1	1
cb eff2	0.992	1	1	1	1
fs eff0	0.865	0.861	0.899	0.880	0.930
fs eff1	0.935	0.935	0.953	0.942	0.967
fs eff2	0.923	0.921	0.944	0.933	0.962
fs calflux	0.054	0.047	0.040	0.054	0.031
fs caldist	1.159	1.307	0.997	1.126	0.758
fs tslew	1.364	1.431	1.287	1.352	1.142
fs tcal	0.172	0.197	0.133	0.169	0.104
fs tcycle	25.14	26.02	30.84	27.67	39.25
fs ttarget	22.09	22.71	27.99	24.68	36.69
fs toverhead	3.086	3.297	2.853	3.030	2.553
fs phase	22.79	23.14	19.35	21.26	15.90
fs atmophase	22.24	22.59	18.69	20.67	15.09
fs gainerror	5.066	5.142	5	5	5
cb calflux	0.152	-1	-1	-1	-1
cb tarflux	0.101	-1	-1	-1	-1
cb caldist	2.257	0	0	0	0
cb tslew	1.862	0	0	0	0
cb tcal	4	0	0	0	0
cb tcycle	300	300	300	300	300
cb ttarget	292.2	300	300	300	300
cb toverhead	7.727	0	0	0	0
cb phase	6.851	0	0	0	0
cb atmophase	6.718	0	0	0	0
cb gainerror	2.239	0	0	0	0
same cal	0.357	0	0	0	0

Table 4: Median fast switching results for 140, 90, 70, and 35 GHz, giving the best conditions to the high frequencies. Frequencies 90 GHz and lower use the target frequency for the calibration frequency.

targetfreq	875	937
calfreq	90	90
el	60	60
tau225	0.0296	0.0296
rms300	0.927	0.927
all phase	37.964	39.815
all eff0	0.6756	0.6431
all eff1	0.8424	0.8220
all eff2	0.8029	0.7854
cb eff0	0.9419	0.9262
cb eff1	0.9676	0.9554
cb eff2	0.9731	0.9691
fs eff0	0.7198	0.6996
fs eff1	0.8660	0.8660
fs eff2	0.8248	0.8102
fs calflux	0.1279	0.1293
fs caldist	1.8785	1.8769
fs tslew	1.6931	1.6962
fs tcal	0.4267	0.4296
fs tcycle	16.623	16.095
fs ttarget	12.671	11.829
fs toverhead	4.0532	4.0730
fs phase	35.558	37.165
fs atmophase	35.205	36.827
fs gainerror	7.9019	8.2590
cb calflux	1.2460	1.3723
cb tarflux	0.3394	0.3680
cb caldist	12.135	14.203
cb tslew	5.9374	6.9506
cb tcal	4	12
cb tcycle	300	300
cb ttarget	280.90	273.89
cb toverhead	19.095	26.108
cb phase	13.360	14.346
cb atmophase	12.719	13.620
cb gainerror	4.2397	4.5401
same cal	0.04	0.025

Table 5: Median fast switching results for 5th percentile conditions, which will be used to set specifications.

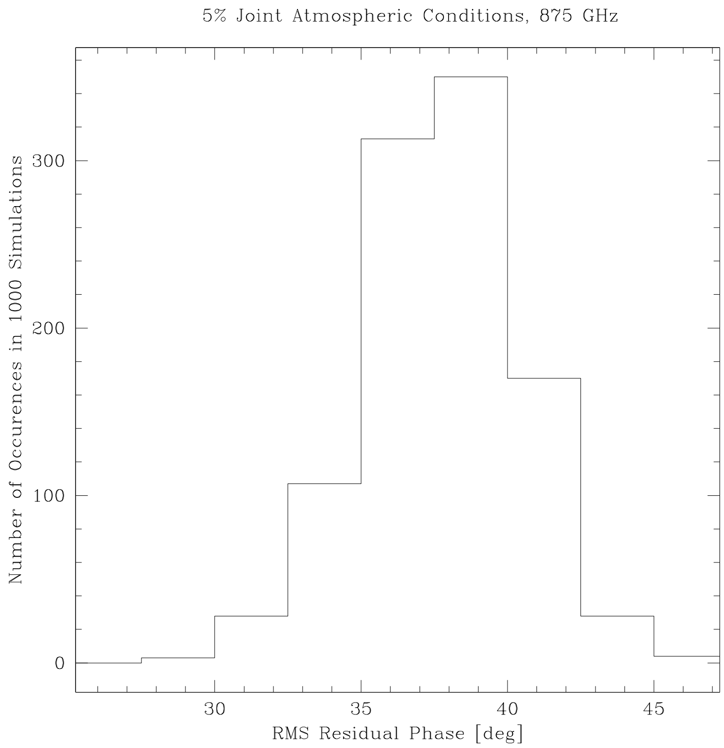

Figure 5: Histogram of the residual phase rms for the simulations reprted on in Table 5 at 875 GHz.

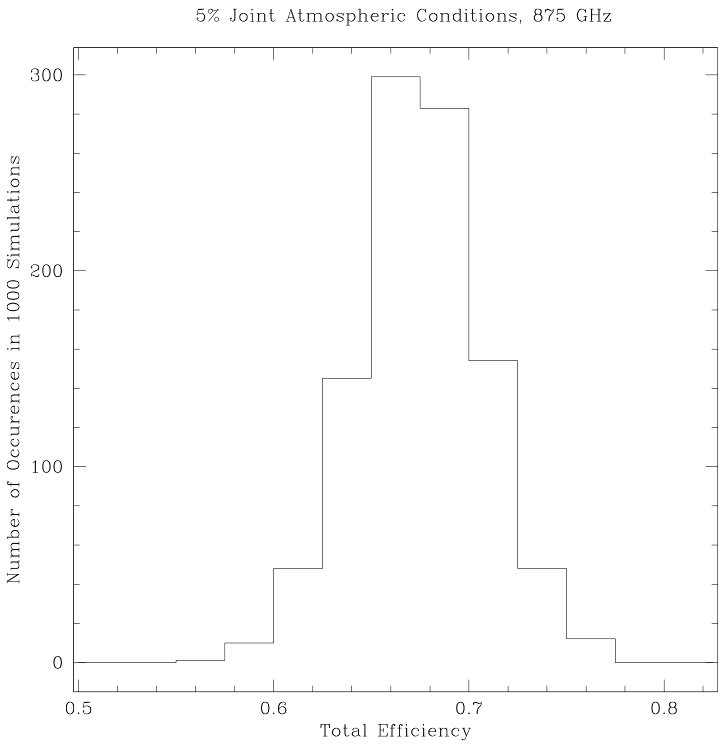

Figure 6: Histogram of the overall efficiency for the simulations reprted on in Table 5 at 875 GHz.

Holdaway, M.A., F.N. Owen, and M.P. Rupen, 1994, "Source Counts at 90 GHz", ALMA Memo 123.

Holdaway, M.A., Simon J.E. Radford, F.N. Owen, and Scott M. Foster, 1995. "Data Processing for Site Test Interferometers", ALMA Memo 129.

Holdaway, M.A., 1996, "Calibration of Submillimeter Observations with SiO Masers: Does the MMA Need Dual Band Capability?", ALMA Memo 148.

Patniak, whenever

Radford, STI paper